Electronic Supplementary Material (ESI) for Analyst.

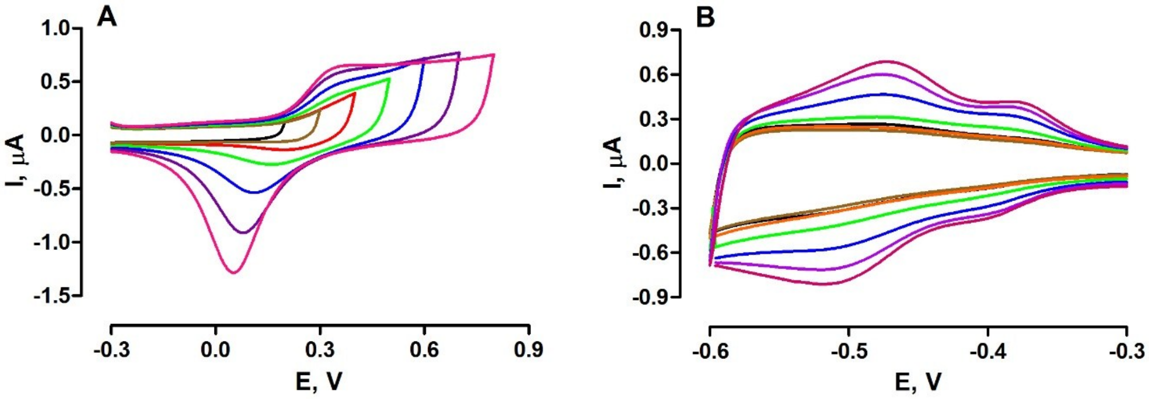

Figure 1S: (A) Effect of increasing oxidation potential on MO reduction peak and (B) subsequent H_2 peaks. Overlay of CVs performed over ranges between -0.65 V to +0.2/0.8 V *vs.* SCE at 100 mVsec^{-1} in nitrogen (N_2) saturated PBS (pH 7.4) at 25°C. Cycle 10 included for each CV.

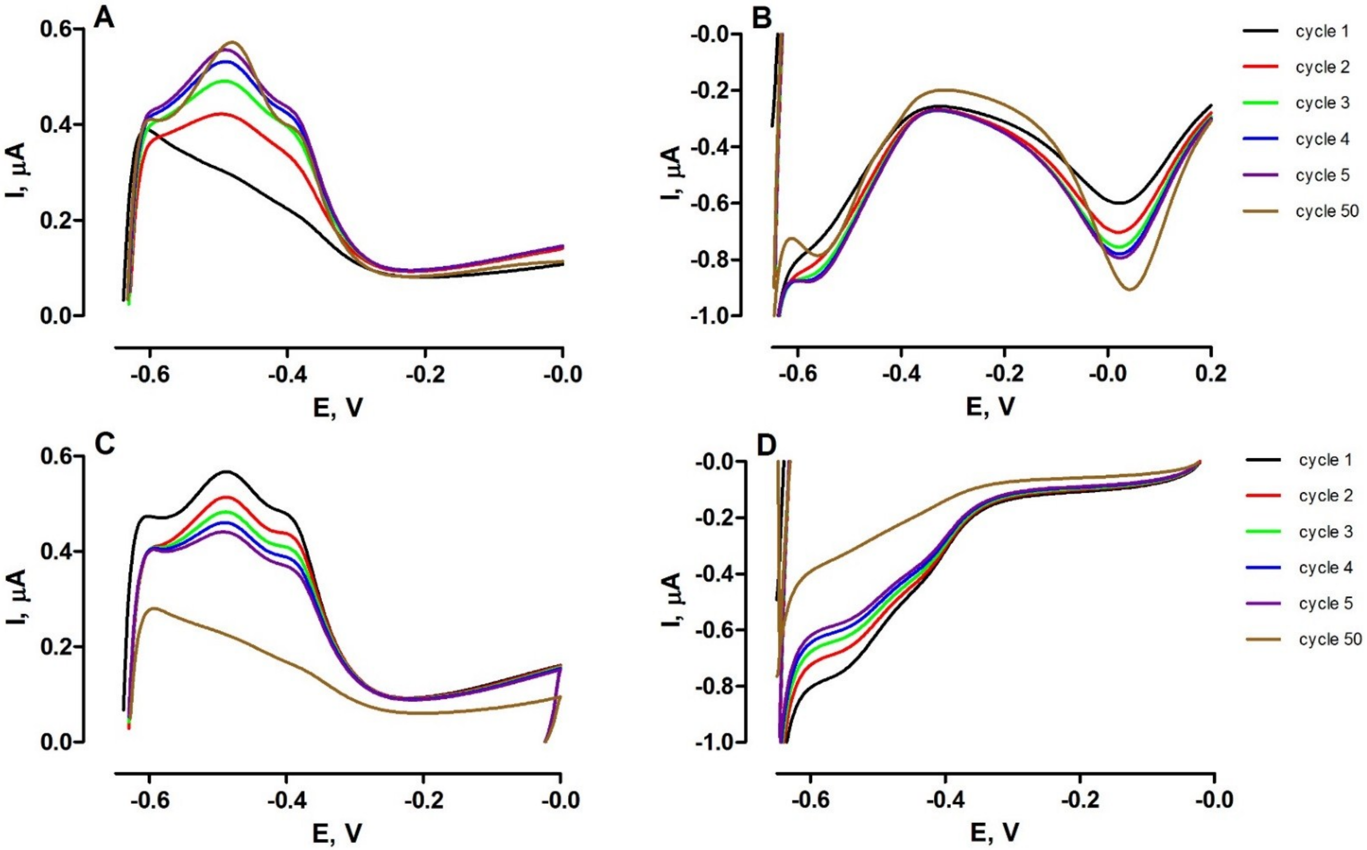

Figure 2S: **Effect of inducing Pt oxidation on (A) H_2 desorption peaks and (B) MO and H_2 adsorption peaks. Overlay of CVs (1-5 and 50) performed over -0.65 V to + 0.8 V *vs.* SCE at 100 mVsec^{-1} in N_2 saturated PBS (pH 7.4) at 25°C (*n* = 4). Subsequent effect of eliminating Pt oxidation on (C) H_2 desorption peaks and (D) MO and H_2 adsorption peaks. Overlay of CVs (1-5 and 50) performed over -0.65 V to + 0.0 V *vs.* SCE at 100 mVsec^{-1} in N_2 saturated PBS (pH 7.4) at 25°C (*n* = 4).**

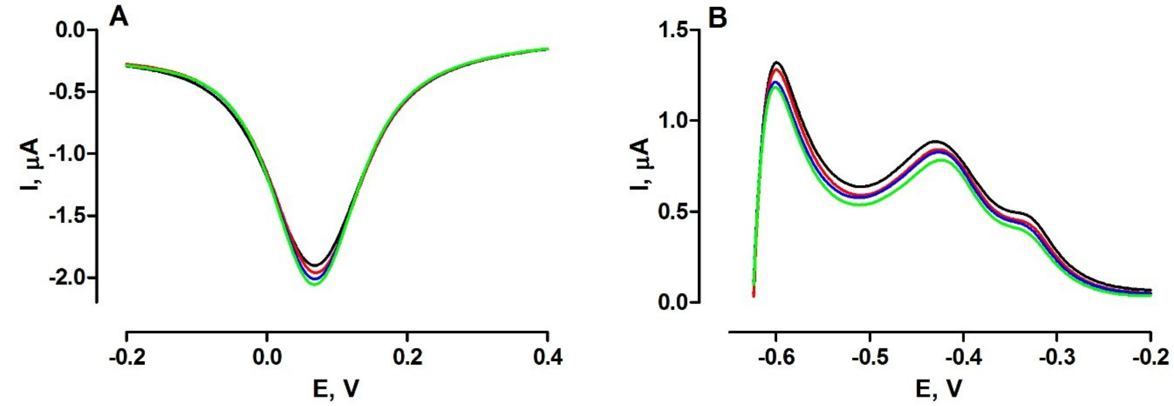

Figure S3: Typical example of a CV performed on 1 mm Pt cylinder electrode in PBS (pH 7.4) at 25°C. performed over range - -0.65 V to +1.0 V *vs.* PRE at 100 mVsec^{-1}. Cycle 50 included for each CV. Stability of (A) MO and (B) H_2 peaks over cycles 50 (black trace), 100 (red trace), 150 (blue trace) and 200 (green trace).

Table S1: Effect of incorporating Ag pseudo reference electrode (PRE) on sensitivity and linearity

PRE	**Sensitivity mVpH^{-1}**	**Linearity (r^2)**
Ag – H_2, cycle 50 (*n* = 9)	81 ± 24	0.92
Ag – MO, cycle 50 (*n* = 9)	119 ± 33	0.93
Ag – H_2, cycle 200 (*n* = 9)	75 ± 11	0.98
Ag – MO, cycle 200 (*n* = 9)	149 ± 10	0.99

Table S1 summarises the effect of incorporating a Ag-PRE into the electrochemical cell. All Pt electrodes were pre-treated in HCL prior to cycling in PBS. It is apparent that its inclusion has compromised the reproducibility of both H_2 and MO peaks with large errors evident between electrodes. The peak potentials recorded for the MO reduction and H_2 desorption peaks were; pH 7.2: 45 ± 17 mV (*n* = 9), pH 7.4: 9 ± 14 mV (*n* = 9), pH 7.6: -3 ± 19 mV (*n* = 9) and pH 7.2: -452 ± 14 mV (*n* = 9), pH 7.4: -476 ± 6 mV (*n* = 9), pH 7.6: -484 ± 15 mV (*n* = 9) respectively. Furthermore, a compromise in linearity and non-Nernstian behaviour was observed for both peaks (MO; 119 ± 33 mVpH^{-1}, *n* = 9, $r^2 = 0.93$ and H_2; 81 ± 24 mVpH^{-1}, *n* = 9, $r^2 = 0.92$). The impact of increasing cycle number from 50 to 200 was investigated to determine if conditioning the electrode surface for longer periods between anodic and cathodic potentials improved these parameters. Figure 3SA and 3SB illustrate typical examples of MO and H_2 reduction peaks at cycles 50, 100, 150 and 200. A slight drift in peak potential for both MO and H_2 was observed between cycle 50 and 100 but the potential appeared to stabilise between cycles 100 – 200. The peak potentials recorded at cycle 200 for the MO reduction and H_2 desorption peaks were; pH 7.2: 57 ± 17 mV (*n* = 9), pH 7.4: 24 ± 6 mV (*n* = 9, pH 7.6: -2 ± 17 mV (*n* = 9) and pH 7.2: -452 ± 16 mV (*n* = 9), pH 7.4: -471 ± 6 mV (*n* = 9), pH 7.6: -482 ± 14 mV (*n* = 9) respectively. Table 1 indicates an improved linearity and a reduction in error at cycle 200. An exaggerated super-Nernstian response was still evident for both peaks (MO; 149 ± 10 mVpH^{-1}, *n* = 9, $r^2 = 0.99$ and H_2 75 ± 11 mVpH^{-1}, *n* = 9, $r^2 = 0.98$).